Electrophilic Fluorination

Deutsche Ausgabe: DOI: 10.1002/ange.201503116
Internationale Ausgabe: DOI: 10.1002/anie.201503116

Selective Aryl–Fluoride Reductive Elimination from a Platinum(IV) Complex**

Ina Dubinsky-Davidchik, Israel Goldberg, Arkadi Vigalok, and Andrei N. Vedernikov**

Abstract: *A difluoro(mesityl)platinum(IV) complex underwent highly selective reductive elimination of 2-fluoromesitylene upon heating in toluene. Kinetic analysis and DFT calculations suggest that the C–F coupling involves a five-coordinate Pt^{IV} transient intermediate resulting from the rate-limiting dissociation of the pyridine ligand.*

Electrophilic fluorination of organometallic complexes of transition metals often involves the formation of high-valent metal species, which in turn undergo reductive elimination.[1] In recent years, such a reaction sequence has been widely used for making new C–X bonds (X = halogen, O, N, C).[2] Of these reactions, the reductive elimination of carbon–fluorine bonds is perhaps the most attractive because of both the importance of organofluorine compounds in industry[3] and the scarcity of synthetic alternatives for constructing such bonds.[4] Aryl–F reductive elimination is a particularly challenging reaction that has received considerable attention with regard to the catalytic fluorination of non-activated aromatic compounds.[5,6] With the notable exception of the Buchwald Pd^0/Pd^{II} catalytic cycle,[7] the majority of catalytic aromatic fluorination reactions involve aryl–F reductive elimination from a late transition metal in a high oxidation state and usually rely on a directing group in the *ortho* position.[8] Importantly, analysis of previously reported examples of aryl–F reductive elimination suggests that it is the least kinetically competitive elimination reaction.[9] Recently, Sanford and co-workers showed the concurrent formation of C–N, $C(sp^3)$–F, and $C(sp^3)$–$C(sp^2)$ bonds from a Pd^{IV} complex with alkyl, aryl, sulfonamide, and fluoro ligands.[10] Aryl–fluoride reductive-elimination products were not formed under the reported conditions. The same research group also described competitive $C(sp^3)$–F and $C(sp^3)$–O reductive elimination from aryl alkyl palladium(IV) complexes, provided the O ligand was a weak nucleophile (O–NO_2 or O–Tos, but not OPh or OAc).[11] Again, no aryl–F bond was formed in those reactions. Finally, Mirica and co-workers recently studied analogous Pd^{IV} complexes; they reported an aryl–OH reductive elimination from a hydroxopalladium(IV) species, but no aryl–fluorine bond formation was observed for its fluoro analogue.[12] Herein, we present the first example of exclusive C(aryl)–F reductive elimination from an isolated aryl platinum(IV) complex from which both aryl–O and aryl–F reductive-elimination reactions might be viable.

Previously, while probing the viability of aryl–F bond formation upon the electrophilic fluorination of diaryl platinum(II) complexes with XeF_2,[5b,13] we found that a competing aryl–aryl elimination from the Pt^{IV} intermediates is by far the predominant path. To exclude the possibility of a C–C coupling reaction, we designed and prepared the new cyclometalated monoaryl Pt^{II} complexes **1a–c** supported by a very bulky anionic P,O chelating ligand (Scheme 1). We hypothesized that the C–F reductive elimination of the aryl platinum(IV) difluorides derived from **1a–c** could be favored by the steric bulk of the ligand over their C–O elimination. Complexes **1a–c** were characterized by multinuclear NMR spectroscopic techniques and, in the case of **1a** and **1c**, also by X-ray crystallography (see Figure S1 in the Supporting Information).

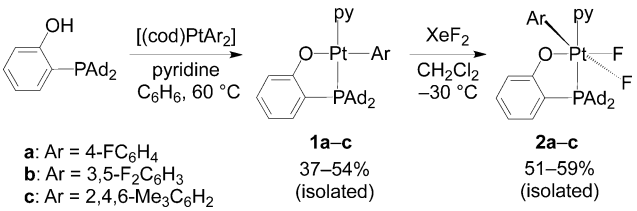

Scheme 1. Synthesis of O-metalated aryl platinum complexes **1** and **2**. Ad = adamantyl, cod = 1,5-cyclooctadiene, py = pyridine.

Complexes **1a–c** reacted with XeF_2 in CH_2Cl_2 to give the corresponding platinum(IV) difluorides **2a–c** (Scheme 1). The fluoro ligands are *trans* to the phenoxo and aryl groups (see below), thus giving very distinct signals in the ^{19}F NMR spectra of **2**. In contrast to the selective formation of **2a**,**b**, the formation of **2c** was accompanied by minor benzylic C–H fluorination of the aryl ligand to give **3** and HF (Scheme 2), so that **2c** appeared as the HF adduct. The competing C–H fluorination could be fully suppressed by the use of CH_3CN–CH_2Cl_2 mixtures (1:5–1:1 ratio). Conversely, in C_6H_5Cl or C_6H_5Cl–toluene mixtures, **2c**·HF and the fluoride **3** were formed in an approximately 1:1 ratio (Scheme 2).

Complex **2c** was isolated and characterized by NMR spectroscopy and X-ray crystallography (Figure 1). The

[*] I. Dubinsky-Davidchik, Prof. I. Goldberg, Prof. A. Vigalok
School of Chemistry, The Sackler Faculty of Exact Sciences
Tel Aviv University
Tel Aviv 69978 (Israel)
E-mail: avigal@post.tau.ac.il
Prof. A. N. Vedernikov
Department of Chemistry and Biochemistry
University of Maryland
College Park, MD 20742 (USA)
E-mail: avederni@umd.edu

[**] This research was supported by grant 2010119 from the US–Israel Binational Science Foundation.

Supporting information for this article, including complete experimental and computational details, is available on the WWW under http://dx.doi.org/10.1002/anie.201503116.

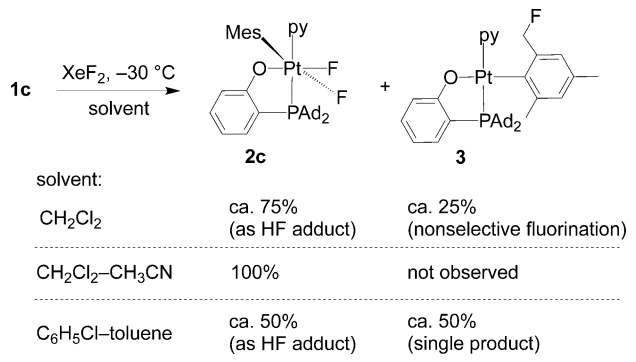

Scheme 2. Competitive oxidative addition–benzylic C–H fluorination of the mesityl complex **1c**. Mes = mesityl.

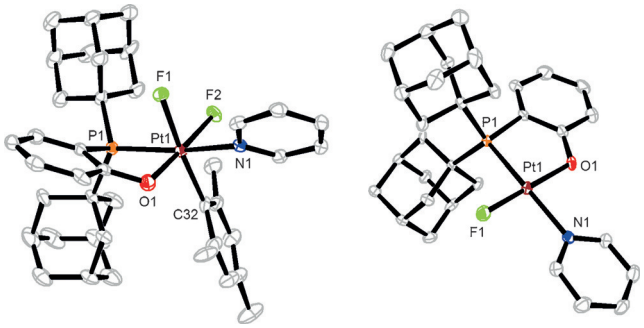

Figure 1. X-ray crystal structures of complexes **2c** (left) and **4** (right). Hydrogen atoms are omitted for clarity. Selected bond distances [Å] and angles [°]: **2c**: Pt1–F1 2.043(2), Pt1–F2 1.963(2), Pt1–O1 1.998(2), Pt1–C32 2.084(4), Pt1–N1 2.119(3); F2-Pt1-F1 88.68(9), F2-Pt1-C32 89.50(12), O1-Pt1-P1 82.28(7); **4**: Pt1–F1 1.987(4), Pt1–O1 1.990(5); O1-Pt1-P1 86.02(14), F1-Pt1-N1 87.55(19).

crystal structure revealed the Pt^{IV} center in an octahedral environment with Pt–F1 and Pt–F2 distances of 2.043(2) and 1.963(2) Å, respectively. These data are in agreement with a stronger *trans* influence of the aryl group as compared to the phenoxide ligand.

Significantly, whereas **2a**,**b** failed to produce fluoroarenes at elevated temperatures, heating of the mesitylplatinum(IV) difluoride **2c** in toluene at 60–100 °C led to clean elimination of 2-fluoromesitylene and the formation of the Pt^{II} complex **4** (Scheme 3; see also Figure S2).[14] The identity of complex **4** was confirmed by NMR spectroscopy and X-ray crystal-structure analysis (Figure 1). No aryl–O elimination was observed under these conditions. Furthermore, no benzylic fluorination to form **3** took place, thus indicating that this difluoroplatinum(IV) complex is not a reaction intermediate for the C–H fluorination leading to **3** that we observed in the reaction of **1c** with XeF_2 in CH_2Cl_2 or chlorobenzene solvents. To our knowledge, the formation of 2-fluoromesitylene from **2c** is unprecedented; it is the first example of well-defined $C(sp^2)$–F reductive elimination from an isolated Pt^{IV} complex.[15]

Our kinetics study of the Mes–F reductive elimination from **2c** revealed the first-order behavior of the reaction, which has the following reaction-activation parameters: $\Delta H^{\ddagger} = (25.3 \pm 1.3)$ kcal mol^{-1} and $\Delta S^{\ddagger} = (2.5 \pm 0.3)$ cal K^{-1} mol^{-1} (Figure 2; see also Figure S3). The addition of pyridine (20 equiv) did not decrease the reaction rate.

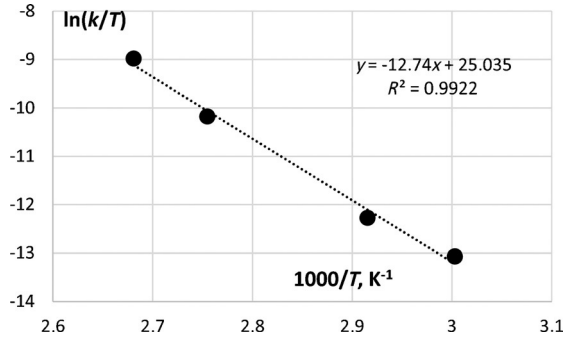

Figure 2. Eyring plot for the reductive elimination of 2-fluoromesitylene from complex **2c**.

Some cationic monofluoropalladium(IV) complexes were found to be significantly more reactive in aryl–F elimination than the corresponding neutral difluoropalladium(IV) analogues owing to more readily generated coordinative unsaturation.[15] Although facile F^- dissociation from **2c** appears unlikely in nonpolar toluene, we decided to independently prepare a cationic monofluoro analogue of **2c** and study its reactivity toward C–F elimination. The treatment of **1c** with Selectfluor (1 equiv) gave an unstable product lacking a signal for platinum-bound fluorine in the ^{19}F NMR spectrum. No reaction was observed between **1c** and the bulky *N*-fluoro-2,4,6-collidinium cation. The reaction between *N*-fluoropyridinium tetrafluoroborate and **1c** gave a mixture of two complexes that showed signals for the platinum-bound fluorine atom, at −298.4 ($J_{Pt,F} = 1149$ Hz) and −310.7 ppm ($J_{Pt,F} = 1442$ Hz), respectively, which were tentatively assigned to cationic **5c-L**, in which **L** is either pyridine or acetonitrile (Scheme 4). Upon the addition of solid CsF, both compounds were slowly converted into **2c**. Heating of the above mixture of **5c-L** as a solution in acetonitrile/toluene or

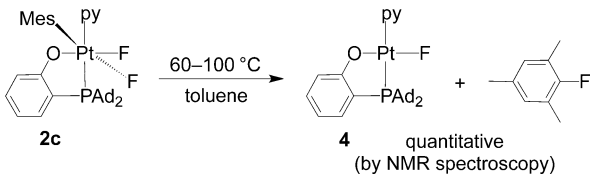

Scheme 3. Selective reductive elimination of 2-fluoromesitylene from **2c**.

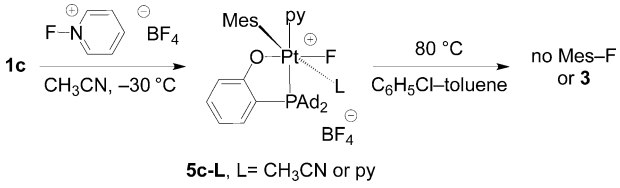

Scheme 4. Synthesis and reactivity of the cationic fluoroplatinum(IV) complex.

the suspension of **5c-L** in chlorobenzene led to decomposition and a complex mixture of products containing neither 2-fluoromesitylene nor **3**. Thus, the cations **5c-L** do not appear to be intermediates in the aryl–F reductive elimination or benzylic C–H fluorination.

To get further insight into the mechanism of the C(sp^2)–F elimination of **2c**, we performed DFT calculations. The resulting Gibbs energy profiles for three potential reaction pathways a–c are given in Figure 3 along with a pictorial representation of the structures of the species involved.

The transition state $\mathbf{TS_{C\text{-}F}2}$ for the direct C–F elimination of **2c** has a prohibitively high energy exceeding 70 kcal mol^{-1} (path a), a significant part of which is needed to arrange the mesityl fragment perpendicular to the Pt-C-F plane. This arrangement is disfavored by one of the 1-adamantyl groups of the bulky P,O chelating ligand present in **2c**. These highly unfavorable interactions are avoided in **6**, the isomer of **2c** with both fluorine atoms *cis* to the mesityl ligand (path b). In **6**, the steric bulk of the P,O ligand favors the necessary conformation of the Pt–Mes fragment for the C–F coupling involving the fluorine ligand *trans* to the phosphorus atom. The corresponding transition state $\mathbf{TS_{C\text{-}F}6}$ has a low energy of 22.1 kcal mol^{-1}. In spite of these features, path b was excluded from further analysis, since the Gibbs activation energy for the direct isomerization of **2c** to **6** is prohibitively high (40.4 kcal mol^{-1}). An even more facile C–F coupling via the transition state $\mathbf{TS_{C\text{-}F}8}$ (16.4 kcal mol^{-1}) is possible from the five-coordinate transient intermediate **8** (path c), a product of pyridine dissociation from **2c**. Path c shows what we believe is the most likely mechanism of the C–F coupling of **2c**. According to this mechanism, **2c** changes its conformation to form **7** with the mesityl-ring arrangement suitable for the subsequent C–F coupling with the fluorine ligand *trans* to the phosphine. This isomerization proceeds via the low-energy transition state $\mathbf{TS_{iso}7}$. The subsequent rate-limiting dissociation of the pyridine ligand and the migration of a fluoride ligand ($\mathbf{TS_d7}$, 23.0 kcal mol^{-1}) generate the required transient intermediate **8**. Since the following C–F coupling of **8** is much faster than pyridine recoordination to form **7**, the dissociation of pyridine from **7** is virtually irreversible.[16] Remarkably, the Gibbs energy of $\mathbf{TS_d7}$ corresponding to the rate-limiting loss of pyridine is a good match to the experimental Gibbs activation energy for the C–F coupling reaction in Scheme 3 ((24.5 ± 0.2) kcal mol^{-1}).[17] The proposed mechanism (path c) can also readily account for the lack of C–F elimination reactivity of **2a**,**b**, the electron-poorer and less bulky analogues of **2c**. According to our calculations, the barriers for pyridine dissociation from both **2a** and **2b** ($\mathbf{TS_d7a}$, $\mathbf{TS_d7b}$) are 2–3 kcal mol^{-1} higher than that for **2c**.[16] Furthermore, their C–F elimination barriers ($\mathbf{TS_{C\text{-}F}8a}$, $\mathbf{TS_{C\text{-}F}8b}$) are 8–9 kcal mol^{-1} higher than for **2c**, thus reflecting a diminished steric repulsion between their aryl ligands, which lack *ortho* substituents, and other ligands present in **8**. Finally, the lack of the potentially competitive C–O reductive elimination of

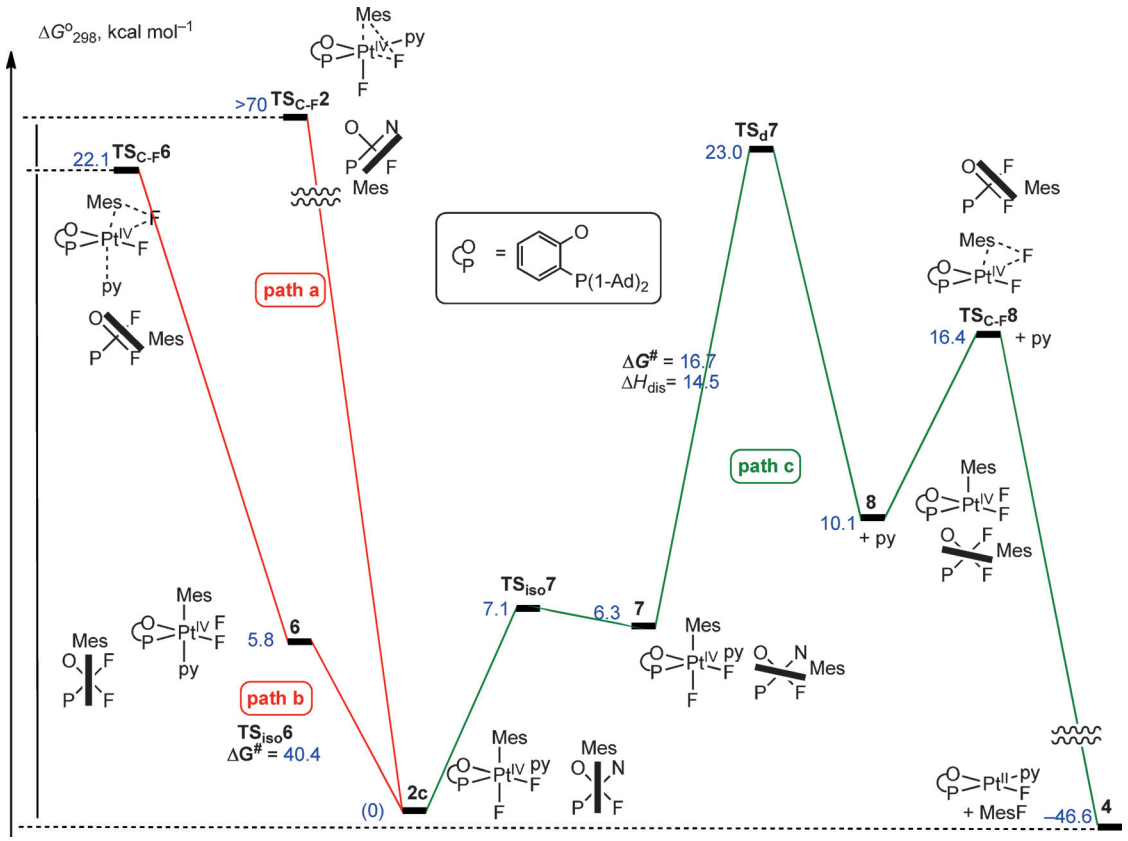

Figure 3. DFT-calculated Gibbs energy profile for potential pathways of the C–F reductive elimination of **2c** in the gas phase. The plane of the mesityl ring is shown with a short bold line.

2c and **8** could be explained by the enormous steric strain that would have to be imposed to achieve the required conformation of the Pt–Mes fragment, that is, to arrange the mesityl ring perpendicular to the Pt-C-O plane. As a result of such structural disparity, the transition states corresponding to the C–O elimination of **2c** or **8** could not be located.

The benzylic fluorination of **1c** to form **3**, an intriguing reaction found during our attempts to convert the Pt^{II} complex **1c** into the Pt^{IV} difluoride **2c** (Scheme 2), was also studied computationally, albeit in less detail (Scheme 5). The

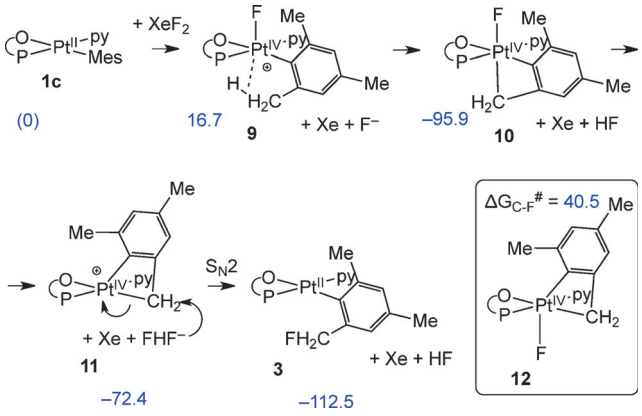

Scheme 5. Proposed mechanism of the benzylic C–H fluorination of **1c** with XeF_2 in CH_2Cl_2. The DFT-calculated standard Gibbs energies of the reactants are shown in blue in kcal mol^{-1} for a solution in CH_2Cl_2.

proposed key intermediate in this case is the C–H agostic Pt^{IV} complex **9**, which is deprotonated by a "naked" fluoride anion to form the benzylplatinum(IV) complex **10**. The latter is converted into the final benzyl fluoride **3** through the loss of a fluoride anion (perhaps in the form of HF_2^- and assisted by HF) and its subsequent S_N2 attack at the benzylic carbon atom of the cationic Pt^{IV} transient intermediate **11**. We also found that the alternative intermediate **12** is unlikely to be involved in the C–F elimination; the Gibbs activation energy for this reaction is prohibitively high at 40.5 kcal mol^{-1}. The calculations are in agreement with our experimental data, which show a significant solvent effect in the formation of **3**. In the presence of coordinating CH_3CN, the formation of an agostic complex **9** should be disfavored, thus suppressing the C–H fluorination pathway. In turn, in more weakly coordinating media, the C–H agostic intermediate **9** would prevail, thus leading to **3**, as we observed experimentally.

In summary, we presented herein the first example of selective aryl–F reductive elimination from an isolated Pt^{IV} complex. In contrast to previously reported similar Pd^{IV} systems, the C(sp^2)–F elimination outcompetes the potentially available C(sp^2)–O pathway, which is disfavored as a result of the enormous steric bulk imposed by a new chelating 2-bis(1-adamantyl)phosphinophenoxide ligand attached to the Pt^{IV} center. Experimental and computational studies suggest that the rate-limiting step of the aryl–F elimination involves the formation of a neutral five-coordinate metal species with subsequent fast C–F coupling. In turn, benzylic C–H fluorination of aryl platinum(II) complexes with XeF_2 occurs via a cationic intermediate "en route" to the aryl platinum(IV) difluoride. Studies of the scope and potential applications of the reaction are currently under way.

Experimental Section

The synthesis and characterization of the new compounds are described in the Supporting Information. In a typical kinetic experiment, a solution of **2c** (10 mg, 0.013 mmol) in toluene (0.5 mL) in a polytetrafluoroethylene liner was heated inside the NMR probe at 60–100 °C, and reaction progress was monitored by ^{19}F NMR spectroscopy by using an internal reference (1,4-difluorobenzene). Only **4** and 2-fluoromesitylene were observed under these conditions. The identity of 2-fluoromesitylene was confirmed by comparison with an authentic sample and by GC.

CCDC 1050345, 1050346, 1050347, and 1050348 contain the supplementary crystallographic data for this paper. These data are provided free of charge by The Cambridge Crystallographic Data Centre.

Keywords: chemoselectivity · electrophilic fluorination · reaction mechanisms · platinum · reductive elimination

How to cite: *Angew. Chem. Int. Ed.* **2015**, *54*, 12447–12451
Angew. Chem. **2015**, *127*, 12624–12628

[1] A. Vigalok, *Organometallics* **2011**, *30*, 4802–4810.
[2] a) A. Vigalok, *Acc. Chem. Res.* **2015**, *48*, 238–247; b) K. M. Engle, T.-S. Mei, X. Wang, J.-Q. Yu, *Angew. Chem. Int. Ed.* **2011**, *50*, 1478–1491; *Angew. Chem.* **2011**, *123*, 1514–1528.
[3] For recent reviews, see: a) J. Wang, M. Sánchez-Roselló, J. L. Aceña, C. del Pozo, A. E. Sorochinsky, S. Fustero, V. A. Soloshonok, H. Liu, *Chem. Rev.* **2014**, *114*, 2432–2506; b) G. Theodoridis, *Adv. Fluorine Sci.* **2006**, 2, 121–175; c) F. Babudri, G. M. Farinola, F. Naso, R. Ragnia, *Chem. Commun.* **2007**, 1003–1022.
[4] For general reviews, see: a) S. D. Taylor, C. C. Kotoris, G. Hum, *Tetrahedron* **1999**, *55*, 12431–12477; b) R. D. Chambers, *Fluorine in Organic Chemistry*, CRC, Boca Raton, FL, **2004**; c) T. Hiyama, *Organofluorine Compounds*, Springer, Berlin, **2000**; d) T. Liang, C. Neumann, T. Ritter, *Angew. Chem. Int. Ed.* **2013**, *52*, 8214–8264; *Angew. Chem.* **2013**, *125*, 8372–8423.
[5] a) T. Furuya, T. Ritter, *J. Am. Chem. Soc.* **2008**, *130*, 10060–10061; b) A. W. Kaspi, A. Yahav-Levi, I. Goldberg, A. Vigalok, *Inorg. Chem.* **2008**, *47*, 5–8; c) N. D. Ball, M. S. Sanford, *J. Am. Chem. Soc.* **2009**, *131*, 3796–3797.
[6] V. V. Grushin, *Acc. Chem. Res.* **2010**, *43*, 160–171.
[7] a) D. A. Watson, M. Su, G. Teverovskiy, Y. Zhang, J. Garcia-Fortanet, T. Kinzel, S. L. Buchwald, *Science* **2009**, *325*, 1661–1664; b) H. G. Lee, P. J. Milner, S. L. Buchwald, *J. Am. Chem. Soc.* **2014**, *136*, 3792–3795.
[8] a) K. L. Hull, W. Q. Anani, M. S. Sanford, *J. Am. Chem. Soc.* **2006**, *128*, 7134–7135; b) X. Wang, T.-S. Mei, J.-Q. Yu, *J. Am. Chem. Soc.* **2009**, *131*, 7520–7521; c) K. S. L. Chan, M. Wasa, X. Wang, J.-Q. Yu, *Angew. Chem. Int. Ed.* **2011**, *50*, 9081–9084; *Angew. Chem.* **2011**, *123*, 9247–9250; d) S.-J. Lou, D.-Q. Xu, Z.-Y. Xu, *Angew. Chem. Int. Ed.* **2014**, *53*, 10330–10335; *Angew. Chem.* **2014**, *126*, 10498–10503; e) for a recent review, see: Y. Li, Y. Wu, G.-S. Li, X.-S. Wang, *Adv. Synth. Catal.* **2014**, *356*, 1412–1418.
[9] We did not find reported examples of aryl–F reductive elimination reactions that compete successfully with other elimination pathways, including alkyl–F reductive elimination; see, for example: J. M. Racowski, B. G. Gary, M. S. Sanford, *Angew. Chem. Int. Ed.* **2012**, *51*, 3414–3417; *Angew. Chem.* **2012**, *124*, 3470–3473.

[10] M. H. Pérez-Temprano, J. M. Racowski, J. W. Kampf, M. S. Sanford, *J. Am. Chem. Soc.* **2014**, *136*, 4097 – 4100.
[11] N. M. Camasso, M. H. Pérez-Temprano, M. S. Sanford, *J. Am. Chem. Soc.* **2014**, *136*, 12771 – 12775.
[12] F. Qu, J. R. Khusnutdinova, N. P. Rath, L. M. Mirica, *Chem. Commun.* **2014**, *50*, 3036 – 3039.
[13] a) A. Yahav, I. Goldberg, A. Vigalok, *J. Am. Chem. Soc.* **2003**, *125*, 13634 – 13635; b) A. W. Kaspi, I. Goldberg, A. Vigalok, *J. Am. Chem. Soc.* **2010**, *132*, 10626 – 10627; c) I. S. Dubinsky-Davidchik, I. Goldberg, A. Vigalok, A. N. Vedernikov, *Chem. Commun.* **2013**, *49*, 3446 – 3448.
[14] The steric bulk of the aryl ligand is important for the formation of a C–F bond: S. B. Zhao, R. Y. Wang, H. Nguyen, J. J. Becker, M. R. Gagné, *Chem. Commun.* **2012**, *48*, 443 – 445.
[15] For aryl–F elimination from an isolated Pd^{IV} complex, see: T. Furuya, D. Benitez, E. Tkatchouk, A. E. Strom, P. Tang, W. A. Goddard III, T. Ritter, *J. Am. Chem. Soc.* **2010**, *132*, 3793 – 3807.
[16] See the Supporting Information for more details.
[17] An alternative reaction sequence leading from **2c** to **8** that involves the rate-limiting dissociation of the pyridine ligand from **2c** first, with subsequent isomerization of the resulting five-coordinate Pt^{IV} transient intermediate, was also analyzed (see the Supporting Information). Our estimate of the Gibbs activation energy for this reaction sequence is 31.0 kcal mol^{-1}.

Received: April 5, 2015
Revised: May 20, 2015
Published online: June 19, 2015

